Characteristics of Porous Beds and Structures

R. B. MACMULLIN and G. A. MUCCINI

The structure of a porous body can be characterized by three parameters, each of which can be directly measured by simple experimental procedures. These parameters are hydraulic radius m, viscous-flow permeability P, and electrical-resistivity ratio R/R_0, which are shown to be related by the simple equation

$$m^2 = k \cdot P \cdot R/R_0 \qquad (1)$$

or, in dimensionless terms,

$$\frac{m^2}{P} = k \cdot \frac{R}{R_0} \qquad (1a)$$

For beds of loose particles of known size and shapes, the hydraulic radius m may be calculated from the relation $m = \epsilon/s$, where ϵ is the void fraction and s the specific surface of the bed. Since this method is not usually applicable to consolidated beds, an experimental procedure based on surface-tension phenomena has been tested. This method, known as the *break point* for granular beds, or *bubble point* for consolidated beds, gives m directly by the relation $m = \gamma/(\Delta p \cdot g)$ where γ is the surface tension of the liquid employed and Δp the pressure required to break through the film of sealing liquid. The sealing liquid must easily wet the porous medium.

The permeability coefficient P is a property of the porous medium only and is evaluated by measuring the resistance to viscous fluid flow by means of a fluid of known viscosity; that is, $P = (u \cdot L \cdot \eta)/(\Delta p \cdot g)$, where u is the superficial fluid velocity, η is the viscosity, and $\Delta p/L$ the pressure gradient.

The resistivity ratio R/R_0 is measured by saturating the specimen with an electrically conducting fluid. R is the resistance in ohms, and R_0 is the resistance of the fluid occupying the same bounds of space as the specimen.

The correlation was tested on a great variety of porous media, including beds of glass beads; sand; and such materials as bonded alumina, porcelain, carbon and graphite, fritted glass, sandstone, and polyvinyl chloride sheet. The mean value of k was found to be 3.666 ± 0.098. The probable error of a single set was found to be 0.65, or 17.6%. Covering a thousand-fold range of hydraulic radius (a million-fold range in permeability), the correlation applies to a wide range of porous media, including packed granular beds and both rigid and flexible consolidated media. The correlation is independent of the porosity, which covers the range of $\epsilon = 0.1$ to 0.85. These are advantages which appear to be lacking in previous correlations by others.

Beyond the viscous-flow range of permeability the following modified forms of the Reynolds number Re and friction factor f are suggested:

$$Re = \frac{m \cdot u_e \cdot \rho}{\eta} = \frac{m \cdot u \cdot \rho}{\eta}\left(\frac{R/R_0}{\epsilon}\right)^{1/2} \qquad (28)$$

$$f = \frac{m \cdot \Delta p \cdot g}{u^2 \cdot L \cdot \rho} \cdot \frac{\epsilon^{1/2}}{(R/R_0)^{3/2}} \qquad (37)$$

The critical Reynolds number Re_{crit}, beyond which the fluid flow cannot be considered as 100% viscous, is approximately $Re_{crit} = 5.5$.

Table A. Fields of Interest in Porous Media

Civil engineering
- Permeability of earth and sand structures, such as dams, subsoil drainage systems
- Flow of wells from water-bearing formations
- Intrusion of sea water in coastal areas
- Filter beds for water supply and sewage purification
- Aeration media for sewage

Geological and mining engineering
- Fluid flow in gas- and petroleum-bearing formations
- Geophysical prospecting by electrical conductivity method
- Leaching of ores and concentrates

Chemical engineering
- Filtration of gases and liquids
- Fluid flow through packed beds
- Gas diffusion and dispersion

Electrochemical engineering
- Permeable and semipermeable diaphragms for electrolytic cells

Medicine and biochemistry
- Biochemical filters
- Mechanical devices to simulate natural organs of the body with respect to fluid flow and electrical response
- Electro osmosis

Miscellaneous
- All industries engaged in manufacture of porous media, such as ceramic, metallic, plastic, rubber, leather, textile, etc.
- Agriculture, as in porous character of soil

THEORY

This paper is concerned with the correlation of viscous-flow permeability and electrical conductivity of porous media. It is believed that such a correlation would be of interest and importance in many fields of technology, as listed in Table A.

Permeability Alone

The most generally accepted concepts of fluid flow through porous beds are based on the Kozeny-Carman (*6* to *9*) equations, which relate the pressure gradient dp/dL of a fluid of density ρ, viscosity η, and superficial (approach) velocity u to the porosity ϵ and specific surface s of a bed of granular, nonconsolidated particles. Various forms of these equations are

$$\frac{dp}{dL} = \frac{fs\rho u^2}{g\epsilon^3} \qquad (2)$$

$$Re = \frac{\rho u}{\eta s} \qquad (3)$$

In terms of average-particle diameter and sphericity ϕ,

$$\frac{dp}{dL} = \frac{6f\rho u^2(1-\epsilon)}{g\phi D\epsilon^3} \qquad (4)$$

$$Re = \frac{\phi D u \rho}{6\eta(1-\epsilon)} \qquad (5)$$

In the viscous-flow region, with $P = (u \cdot L \cdot \eta)/(\Delta p \cdot g)$

$$f = \frac{k_c}{Re} = \frac{5}{Re} \qquad (6)$$

$$m^2 = k_c \frac{P}{\epsilon} \qquad (7)$$

• The coefficient k_c is variously reported as from 5 to 5.5.

Useful as these equations may be, their limitations are often overlooked. For example, the porosity ϵ is an important factor. In loose beds of solid particles of known density, ϵ may be calculated readily enough from the apparent density of the porous bed. In consolidated bodies of such materials as porous ceramics, porous carbon, or sandstone, there are complications. One must distinguish between pores that are open, semiclosed, and closed and between the microporosity contributed by the porous nature of the particles themselves and the macroporosity of the interstitial space around the

R. B. MacMullin is with R. B. MacMullin Associates, Niagara Falls, New York, G. A. Muccini, formerly at Niagara University, Niagara Falls, New York, is now at the University of Notre Dame, South Bend, Indiana.

particles. The porosity to be used in the Kozeny-Carman equations, therefore, is frequently in doubt and sometimes immeasurable.

Likewise, the specific surface s is an important factor. Obviously, the internal surface of microporous particles contributes little or nothing to the resistance to fluid flow, as compared with the external surface of the particles. Even in beds of irregular but nonporous granules the external surfaces sometimes mate, and these surfaces are "blind" to the flow of fluid. The total surface of a porous bed may be determined by the gas-absorption method, but obviously this is not necessarily the specific surface called for in the Kozeny-Carman equations.

The hydraulic radius m of Equation (7) is defined, for a porous body, as the ratio ϵ/s. It is therefore subject to the same sources of error as ϵ and s separately. There is, fortunately, a method that can be used to measure hydraulic radius directly. If a porous body is saturated with a liquid which easily wets the body, the liquid is locked into the pores by surface tension forces. In the well-known bubble-pressure method, and also the new breakpoint method described later, the force required to break through this sealing liquid is measured. At the saturation level in the bed, the following forces are in balance over a unit area of bed:

Force supported = open area$\cdot\Delta p\cdot g$

Supporting force = wetted perimeter of grains$\cdot\gamma\cdot\cos\theta$

The ratio, open area/wetted perimeter = hydraulic radius m

$$\therefore\ m = \frac{\gamma\cos\theta}{\Delta p\cdot g} \qquad (8)$$

If this is true for any section of the bed, it is true for all sections of the bed, provided that (a) the structure of the bed is reasonably (or better, statistically) uniform and (b) the unit area chosen is much larger than the areas of the open pores. By proper choice of sealing fluid, cos θ may be taken as unity. Hence

$$m = \frac{\text{open area} \times L}{\text{wetted perimeter} \times L} = \frac{\epsilon}{s} \qquad (9)$$

Equation (8) is also used as the basis for determining "pore-size" distribution in a porous body, sometimes by use of mercury or some nonwetting liquid. Opinion varies as to whether m, given by Equation (8) by the bubble-point method, is identical with the reciprocal average value of m as calculated from the distribution curve or with the value of m calculated from independent measurement of ϵ and s. In the experiments here reported, the equivalence is quite good. The breakpoint method is believed to selectively exclude closed and semiclosed pores from the numerator of Equation (9), as well as to exclude the blinded surfaces from the denominator. If this is true, the breakpoint method should give the desired value of m to be used in the Kozeny-Carman equation (7). On the other hand, the reciprocal average m calculated from the distribution curve is likely to give undue weight to the very small values of m, which results from forcing the sealing liquid (mercury) into semiclosed pores and micropores.

Entirely aside from the question of what values of m, ϵ, and s to use in the Kozeny-Carman equations is that of the organization of the network of pores, the effective velocity u_e of the fluid in the pores, and the effective length of path L_e of a parcel of fluid. These factors may be lumped under the general heading of *tortuosity*, a term which conceals a great deal of ignorance. If the tortuosity is universal, then the Kozeny-Carman coefficient k_c should be a natural constant. For an illuminating discussion of this point, the reader is referred to a recent article by Scheidegger (*24*), who concludes that the tortuosity can have values in an extremely wide range and that it is not surprising that the Kozeny-Carman relation is frequently in poor agreement with actual experimental results. This emphasizes the danger of extending the very useful Kozeny-Carman equations into regions of application where they were not intended. For treating permeability in consolidated porous bodies, one must therefore search for a key to tortuosity.

It is recognized that much important work in this field has been published since the classical paper of Carman. For granular beds, Brownell and Katz (*2, 3, 4*) introduced arbitrary correction factors in the form of exponents of the porosity. Leva and coworkers (*17*) used the Kozeny-Carman relation to estimate surface of tower packings. Ergun (*14*) considered the problem of mixed flow, partly viscous and partly turbulent, in packed columns, and Wagstaff and Nirmaier (*30*) further verified the Ergun equation. Brownell (*5*) deduced a modification of the Kozeny-Carman equation which applies to beds of spheres consolidated with resin. Tiller (*27, 28*) and Grace (*15*) have applied the Kozeny-Carman relation to the unit operation of filtration, and Whitney (*31*) to the dewatering of wood pulp and fibrous materials. Hatfield (*16*) studied the permeability of porous carbon and graphite. Much information is to be found in books by Dallavalle (*13*), Muskat (*19*), and Terzaghi (*26*). It has become clear that no single general equation based only on the variables used by Kozeny-Carman has yet been proposed that is adequate for such an extensive range of application.

Before leaving this subject, the authors wish to point out an approach that could give permeability solely in terms of porosity and specific surface, provided that the fine structure of the bed is known. This can be done by evaluating the point-to-point variation of the hydraulic radius within the porous structure. Application of the method to certain geometrically predetermined beds is given in the appendix.*

Electrical Resistivity Alone

Electrical-resistivity measurements have been made on many porous nonconducting bodies, the pores being filled with a conducting medium (*1, 10, 11, 17, 18, 21, 22, 29, 32* to *35*). At first one might be tempted to reason that if such a body were, say, 40% porous, then it would conduct 40% as well as if the body were 100% porous (i.e., no solids present at all). This is far from the truth; the resistance always is much higher. The first record that could be found of this discovery was made by Velisek and Vasicek (*29*). To explain this result, they reasoned as follows: Since the pore structure resembles a three-dimensional network, only one of the three dimensions is in a position to conduct, namely, the one coinciding with the direction of the potential gradient. On this basis, $\epsilon\ R/R_0 = 3$. For porous bodies consisting chiefly of fissures, two dimensions conduct, and so $\epsilon\ R/R_0 = 1.5$. These authors were qualitatively correct in their reasoning. In the present work $\epsilon\ R/R_0$ ranged from 1.5 minimum to 3.0 maximum. In some recent work by Cornell and Katz (*11*), $\epsilon\ R/R_0$ ranged from 1.8 to 5.9 for sixteen samples of sandstone, and from 6.1 to 10.7 for eight samples of dolomite and limestone. De LaRue and Tobias (*12*) have recently determined the influence of suspended nonconducting particles on the conductivity of a liquid. The equation that they evolved will be discussed later in relation to the present work.

When a porous body is itself an electrical conductor, the mechanism of conduction is more complicated, as shown by Sauer et al. (*23*). The conductivity of the pore structure, however, can be independly measured by the use of direct current, as will be explained under Experimental Methods. There are other disturbing factors that can influence the measurement of resistivity ratio unless proper conditions are chosen to avoid them. The phenomena of superconductivity at low electrolyte concentration, doubly ionized layers, internal reactance, and such are dealt with in the cited references.

Permeability and Electrical Resistivity Together

A very early attempt to correlate permeability with resistivity ratio was made by Wirth (*32*), who presented an equation that reduces to $m^2 = 2P\cdot R/R_0$. The form of this equation is believed to be correct, but the coefficient 2 derives from the assumption of Poiseuille's law for capillary flow. This is known to give an erroneous result for porous beds.

*Complete data may be obtained as document 4955 from the American Documentation Institute, Photoduplication Service, Library of Congress, Washington 25, D. C., for $2.50 for photoprints or $1.75 for 35-mm. microfilm.

Much work has been done by Wyllie and Gregory (*33*, *34*) and by Cornell and Katz (*11*), all of whom introduce the resistivity ratio as a correction factor for various permeability equations. Cornell and Katz, for example, identify $(L_e/L)^2$ with $\epsilon \cdot R/R_0$ in the ideal form of the Kozeny-Carman equation

$$\frac{dp}{dL} = \frac{k_0 u\eta}{m^2 g\epsilon} \cdot \left(\frac{L_e}{L}\right)^2 \qquad (10)$$

which reduces to

$$m^2 = k_0 PR/R_0 \qquad (11)$$

Two problems remain: (1) the theoretical justification of an equation of the foregoing type and (2) the determination of the coefficient over a wide range of conditions. The present authors have undertaken to solve both problems.

Theoretical Basis for Relating Permeability to Resistivity Ratio

Since fluid velocity in the 100% viscous flow region is characterized by the relation

$$u\eta \sim \epsilon m^2 \chi \text{ grad } p \qquad (12)$$

and electrical current density by the relation

$$I_0(r) \sim \epsilon\chi \text{ grad } E \, . \qquad (13)$$

it can be seen that the phenomena are analogous.

Equation (12) states that the velocity of a fluid of unit viscosity is proportional to the pressure gradient and three determining structural dimensions of the network. These dimensions are porosity ϵ, hydraulic radius squared m^2 (which produces the drag in viscous flow), and tortuosity χ, which is the "fudge" factor introduced to make Darcy's law hold. This equation may be recast into the more familiar form,

$$k\frac{u\eta L}{g\,\Delta p} = kP = \epsilon m^2 \chi \qquad (12a)$$

Equation (13) states that the current flowing through unit area of a specimen the pores of which are filled with a conductor of unit resistivity is proportional to the potential gradient and two determining structural dimensions of the network. These dimensions are porosity ϵ and tortuosity χ, which is precisely the same "fudge" factor used in Equation (31), here introduced to make Ohm's law hold. This equation may be recast into the more familiar form,

$$(r)L = R_0 = \epsilon\chi \frac{E}{I} = \epsilon\chi R \qquad (13a)$$

or

$$R_0/R = \epsilon\chi$$

Combining (31*a*) and (32*a*) so as to

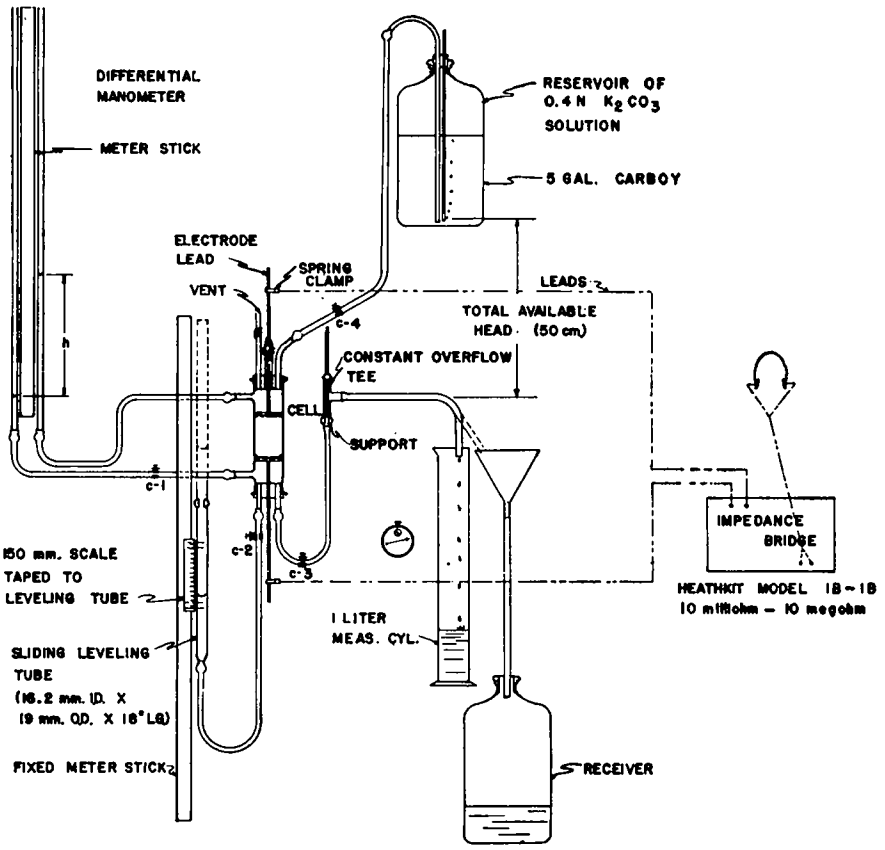

Fig. 1. Assembly for simultaneous measurement of permeability, electrical resistivity, and hydraulic radius of packed beds of unconsolidated particles.

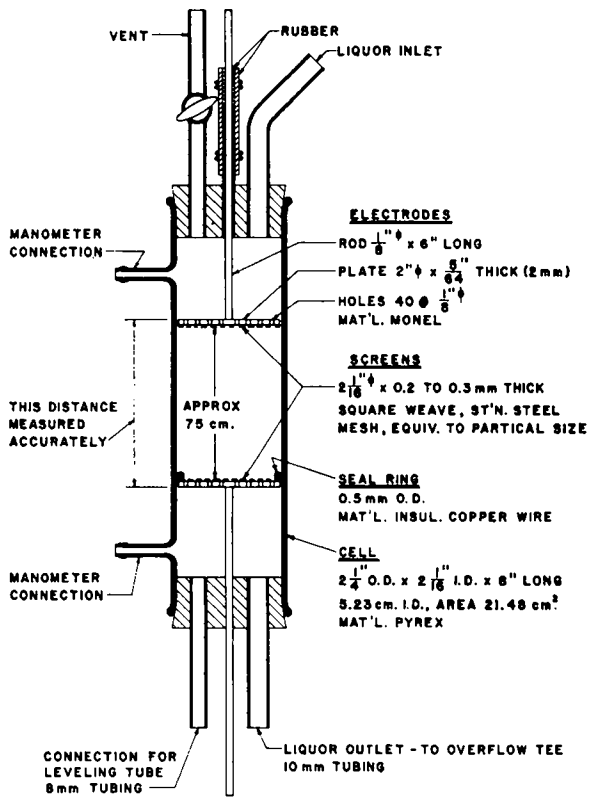

Fig. 2. Details of cell shown in Figure 1 (for unconsolidated beds).

eliminate ϵ and χ, one obtains the simple relation

$$m^2 = kPR/R_0 \qquad (1)$$

To prove this relation is the object of this paper, and therefore, independent measurements of hydraulic radius, permeability, and resistivity ratio have been made.

EXPERIMENTAL METHODS

Unconsolidated Packed Beds

It is of prime importance that the packed bed, once formed, must not in any way be disturbed during the course of the several measurements made upon it. The assembled equipment for accomplishing this is shown in Figure 1. Cell details are shown in Figure 2.

The solution used for the tests was 0.4N K_2CO_3, prepared from Baker's analyzed $K_2CO_3 \cdot H_2O$ crystal and distilled water. This solution was analyzed frequently. This particular electrolyte was chosen for the following reasons: (1) it is available in highly pure form; (2) it is stable to atmospheric air; (3) it has no effect on cell parts, such as pyrex glass, rubber, Tygon, Monel, electrodes, stainless steel screens; (4) it has no effect on the materials tested, glass beads, silica sand; and (5) all the necessary physical properties, such as density, viscosity, surface tension, and electrical resistivity, are accurately known as a function of concentration and temperature within the range of the work. These physical properties are listed in Table 13.*

Materials Tested. Superbrite glass beads were obtained from Minnesota Mining & Minerals Co. in four graded sizes as follows:

Grade No.	U.S. sieve size Through	On
108	40	45
109	50	60
110	60	80
111	100	120

Particle size† 1	2	3	Avg.
392	390	410	397
271	290	325	295
228	200	214	214
136	150	157	148

†1. Reciprocal average of screen opening.
2. Data from company (presumably micrometered).
3. Measured by authors. Average of fifty beads from random sample, measured under microscope with filar micrometer. Over 95% of the beads were perfect spheres, the balance somewhat ellipsoidal.

The glass beads were found to be free of extraneous material. A water extract was substantially as nonconducting as the water used. The specific gravity of the beads was measured and found to be 2.572.

A bag of clean, dry, washed, sized quartz sand of very light color was obtained. A screen analysis on new U. S. standard screens gave the results shown in Figure 12.* This sand was then carefully and exhaustively sized, and two ranges, 40 to 60 and 60 to 80, were selected for testing. Since the plot of accumulative weight fraction against $6/D$ (Figure 12) gave practically a straight line, it follows that the reciprocal average diameter for the chosen cuts truly represents the diameter for which specific surface and sphericity can be calculated. The hydraulic radius and porosity of six different beds were measured by the break-point method and yielded specific surface by the relation

$$s' = \frac{\epsilon}{(1-\epsilon)m}, \text{ sq. cm./cc. of sand} \qquad (14)$$

The specific surface of true spheres of diameter D_{ra} would be $s_0' = 6/D_{ra}$, where D_{ra} is the reciprocal average diameter for the cut. Sphericity is then defined as $\phi = s_0'/s'$.

Five beds of sand gave the accompanying results. The specific gravity of the sand was measured and found to be 2.640.

Preparation of Bed. With the lower electrode, screen, and wire seal ring in place, the cell was partly filled with potash solution, enough to cover the added beads or sand. An accurately weighed amount (approximately 200 to 250 g.) of particles was added slowly through a funnel, the stem of which was swirled above the surface of the liquid. In this way a uniform and level bed is formed, free from trapped air bubbles. The cell is then vibrated to pack the bed, and during that time the upper screen and electrode are placed and pressed down firmly. The cell is then filled and connected to the constant-level feed tank. All air is carefully vented from feed lines and cell. Clamps c-1 and c-3 are opened, and c-2 is closed. The flow of electrolyte is controlled by c-4.

The depth of bed is measured by taking a series of ten readings around the cell. Since the outer edges of the electrodes are clearly visible, this distance is actually measured; from the average value, the calipered thickness of the two electrodes and two screens is subtracted. The inside diameter of the cell is, of course, known.

Permeability. After steady state conditions are reached at any particular flow rate, the overflow is diverted to the liter-measuring cylinder, and the time to fill is measured with a stop watch. At regular intervals the loss in head is taken on the manometer, and the outlet temperature is recorded. Several flow rates are tried, and the proportionality of flow rate to head is checked immediately. Any deviation from proportionality would be cause for rejection of the data as not representing viscous-flow conditions. The correction for pressure drop through the screens has been shown to be negligible.

Permeability is calculated from the equation

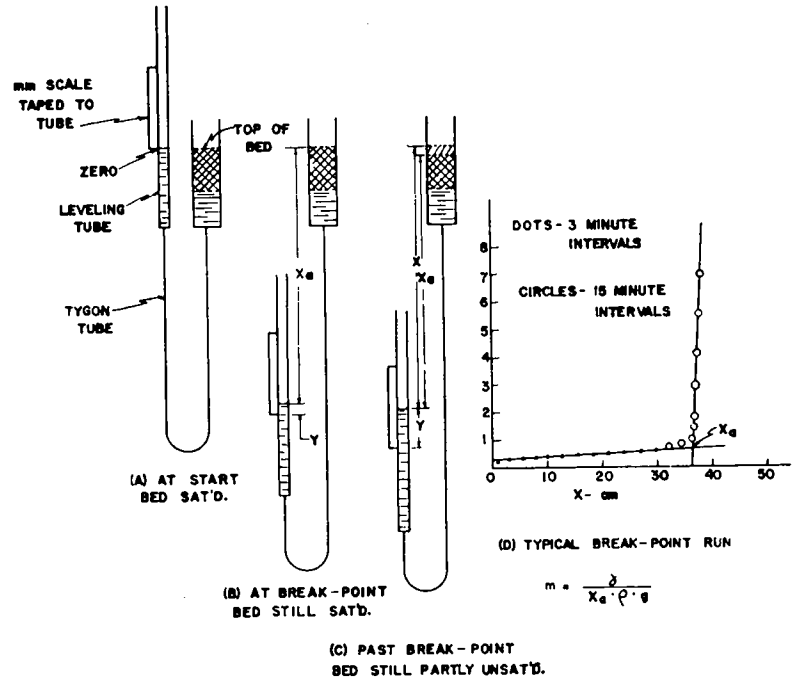

Fig. 3. Principle of break-point method for determining hydraulic radius of packed beds.

Results on Five Beds of Sand

Mesh through/on	D_{ra}, μ	m, μ	ϵ	s' cm.$^{-1}$	s_0' cm.$^{-1}$	ϕ
40/60	315	26.5	0.4423	300	190	0.634
40/60	316	26.8	0.4470	302	190	0.634
40/60	316	27.35	0.4325	281	190	0.677
60/80	207	19.25	0.4450	416.6	290	0.696
60/80	207	18.67	0.4570	450	290	0.645
					Average	0.657

*See footnote on page 394.

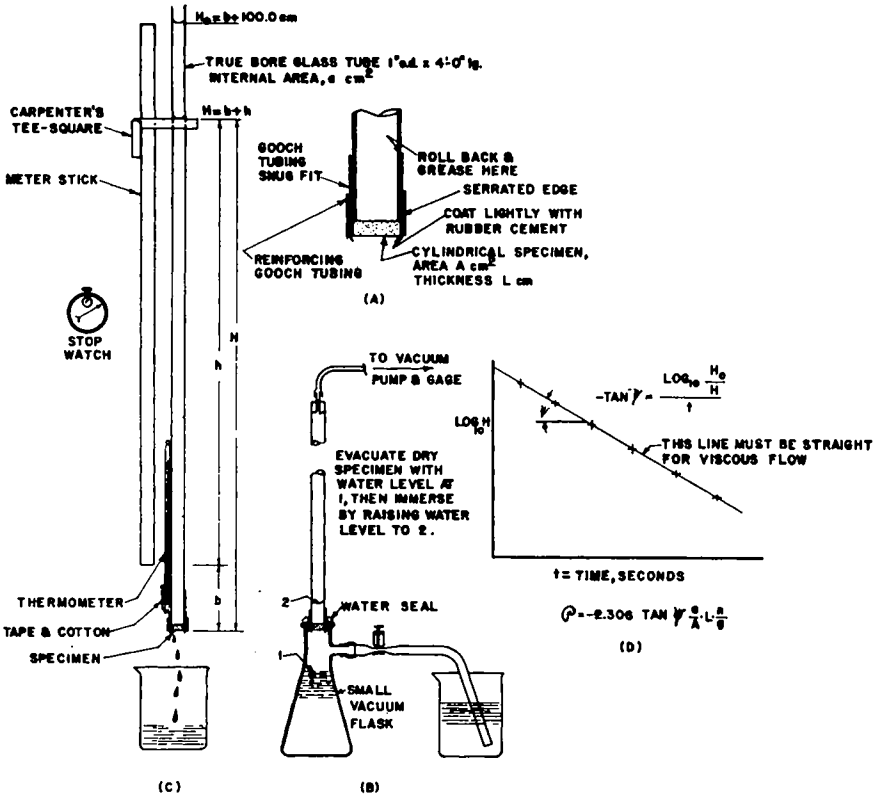

Fig. 4. Water-permeability test, falling-column method.

may seal off some of the pores and give erroneous results; (3) specimens must be thoroughly dry before testing for gas permeability; (4) specimens must be freed of entrapped air (by evacuation) in order to obtain 100% saturation with liquid before testing for liquid permeability or resistivity; (5) specimens must be carefully sealed at the edges to prevent by-passing of fluid; and (6) when the bubble-point test is made for hydraulic radius, the fluid chosen should easily wet (have an affinity for) the specimen.

The specimens were prepared in the form of true cylindrical disks, approximately 1 in. in diameter and ¼ in. thick, with faces strictly parallel. All specimens were then accurately calipered.

Materials Tested. Porous porcelain filter disks from the Selas Corporation are made, it is understood, by incorporating carbon in the ceramic mix, so that, on firing, the carbon burns out, leaving a porous structure. The following grades were tested: XF, XFF, 10, 01, 015, 02, and 03.

Grades PC 40 and 60 and PG 40 and 60 of porous carbon and graphite from National Carbon Company were tested. For an estimate of m, based on grain size, distribution, and other data, the results shown in Table 4 should be consulted.

Of fritted-glass filter tubes made by Corning Glass Works and supplied by Will Corporation, three grades were tested, coarse, medium, and fine.

Water Permeability, Falling-column Method. In this method, also known as the method of Terzaghi (*26*), the specimen is lowered 1 cm. at a time at 15-min. intervals. Past the breakpoint, $\Delta y/\Delta x$ increases rapidly. Sufficient points are recorded to fix the slope of the new line accurately. The unsaturation line in the bed is usually clearly visible, because air has been drawn into the bed. It has been found impossible to reverse the procedure and to drive the air out of the bed by raising the leveling tube. It is, therefore, considered impractical to repeat the break-point tests, and it is preferable to start all over.

The intersection of the two lines, as shown in Figure 3(*D*) is considered to be the breakpoint, and x_a gives the effective head of liquid supported by the sand owing to surface tension. Neglecting the angle of contact θ gives

$$m = \frac{\gamma}{x_a \rho g}, \text{ cm.} \qquad (16)$$

Density of Particles. Density was determined by comparing the weight in air and in water by use of a 200-g. sample and taking care to avoid errors due to entrapped air.

$$P = \frac{uL\eta}{\rho\, \Delta h\, g}, \text{ cm}^2 \qquad (15)$$

Resistivity. Simultaneously with the foregoing permeability tests, the resistance R of the bed is taken on the impedance bridge. Sharp null points are obtained, by use of 1,000-cycle current and telephone detection. R_0 is calculated from the dimensions of the bed and the specific resistivity of the solution, on the basis of Ohm's law. The resistance of the electrodes, screens, and leads was measured and found to be negligible.

Hydraulic Radius. At the conclusion of the above-mentioned measurements of permeability and resistivity, and without any disturbance to the bed, the liquid level is dropped to the top of the bed (with the vent open). Clamps c-1, c-3, and c-4 are tightly closed, and c-2 is opened. The leveling tube is then adjusted to the top of the bed. The celluloid millimeter scale is then taped to the leveling tube, with the zero mark at the level of the water.

The leveling tube is then lowered 2 cm. at a time, at 3-min. intervals, and two readings are taken: the position of the zero mark of the millimeter scale with reference to the stationary meter stick and the level of the water in the leveling tube with reference to the millimeter scale. The top of the bed, with reference to the meter stick, is, of course, noted and remains constant.

The distance x and y are calculated and plotted immediately, in the manner shown in Figure 3 (*D*). As the breakpoint is approached, the increment $\Delta y/\Delta x$ starts to increase. At this point the leveling tube is

Rigid Porous Materials

The testing of rigid materials has the intrinsic advantage that the same specimens may be tested over and over again. It is necessary only to take the following precautions: (1) only clear liquids or clean gases may be used, to prevent clogging of the pores with fines; (2) the faces of specimens, particularly the fine ones, must not be handled with the fingers, as grease or wax

Fig. 5. Apparatus for measuring gas permeability of rigid specimens (*a*) by use of rotameters, (*b*) by use of water displacement.

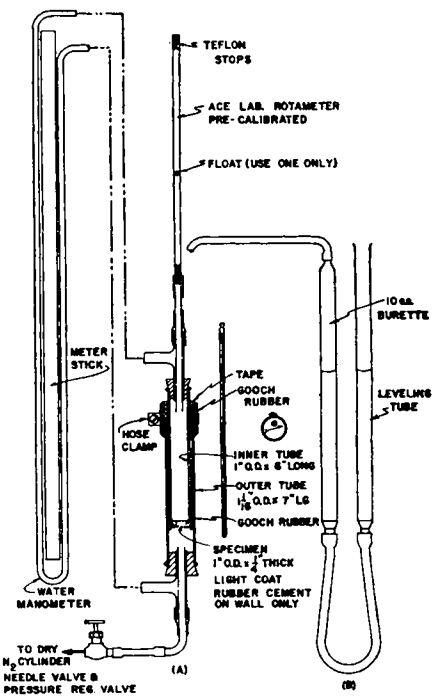

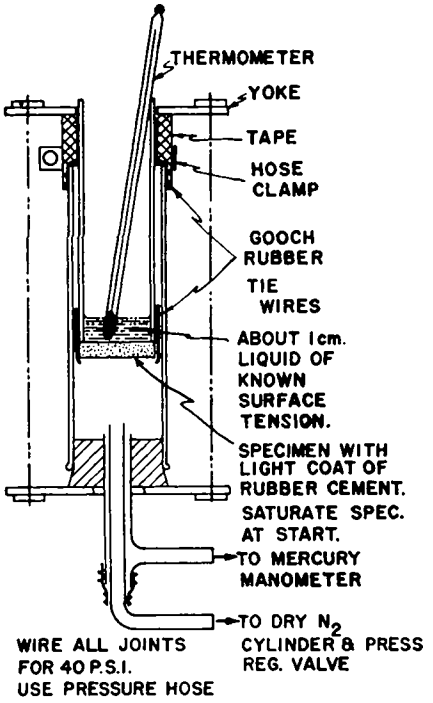

Fig. 6. Apparatus for measuring bubble-point pressure of rigid specimens.

mounted below a column of water, and the height of the water column is measured against time. The inside area of the tube being known, the permeability can be calculated. The apparatus used is shown in Figure 4. Cut A shows how the specimen is mounted, cut B shows how the specimen is evacuated and saturated with water, cut C shows the assembly during test, and cut D shows the method of plotting the data.

If a = area water column, sq. cm.
A = area specimen, sq. cm.
L = thickness of specimen, cm.
H = head of water, cm., at time t, sec.
$\tan \psi$ = slope of line, $\Delta \log_{10} H/\Delta t$

Then $P = -2.306 \tan \psi \, (aL\eta/Ag)$, sq. cm. (17)

For viscous-flow conditions the plot of $\log H$ vs. t must be straight; otherwise, the experiment must be rejected.

Gas Permeability. In this test dry nitrogen gas from a cylinder equipped with a sensitive gas-pressure regulator is passed through the specimen. Pressure drop is measured by water manometer. Gas flow is measured either by a precalibrated Brooks laboratory flow meter (supplied by Ace Glass Company) or by the time required for water displacement from a calibrated pipette. The apparatus is shown in Figure 5. In use of the Brooks flow meter only one float is used, not two, as suggested by the manufacturer. The instruments were recalibrated before use. Moreover, the ball must be handled with care. If it is dropped on the floor, the calibration will change. The usual temperature and pressure corrections are applied to reduce readings to the temperature of the experiment.

For each specimen, several flow rates are used, covering a threefold range. Proportionality between flow rate and pressure drop is proof that the flow is in the viscous range; otherwise the experiment is useless.

If the pressure drop is only a matter of 10 to 40 cm. H_2O head, then the correction for expansion of the gas in the specimen is negligible. Where the pressure drop through the specimen is appreciable, the following correction factor must be applied to each different flow rate, after which the true permeability may be calculated:

$$\text{correction factor } C = \frac{2p_2}{p_1 + p_2} = \frac{2p_2}{2p_2 + \Delta p} \quad (18)$$

where

p_1 is the upstream absolute pressure (cm. of H_2O)
p_2 is the downstream absolute pressure (cm. of H_2O)

$$\Delta p = p_1 - p_2, \text{ cm. of } H_2O$$

$$P = \frac{CuL\eta}{\Delta p \, g}, \text{ sq. cm.} \quad (19)$$

Hydraulic Radius, Bubble-point Method. The specimen is mounted as shown in Figure 6. When mounted, the specimen is covered with about 1 cm. of a liquid of known surface tension which is allowed to permeate. It is not necessary to evacuate the specimen and saturate, as this procedure gives the same result as the simple permeation procedure.

The cell is connected to a dry nitrogen cylinder through a sensitive pressure regulator. The pressure is slowly increased until a slow but steady stream of bubbles is seen rising through the sealing liquid. Any bubbles from the edge do not count, only those arising from some part of the upper surface of the specimen. The bubble pressure is read on a mercury gauge or water gauge as applicable. If the pressure is too high for the mercury gauge, for example 40 cm. of greater, the Bourdon gauge on the low-pressure side of the regulator may be read. The gas pressure is then reduced and the procedure repeated to give a series of readings, which are averaged. Increasing the flow rate through the specimen until gas evolves all over the surface does not increase the bubble-point pressure appreciably. Above a certain point, however, the pressure increases owing to pressure drop through the specimen. With a little practice, the bubble point is reproducible.

It is important to use a sealing fluid that wets the porous body. Water is excellent for glass, porcelain, sandstone and, most ceramic bodies but is useless for porous carbon and graphite. For these materials CCl_4 or C_6H_6 may be used.

The hydraulic radius is calculated from the equation

$$m = \frac{\gamma}{\Delta p \, g}, \text{ cm.}$$

where

γ = surface tension of liquid at temperature of experiment
Δp = bubble-point pressure, cm. H_2O
g = 980.6 cm.sec.$^{-2}$

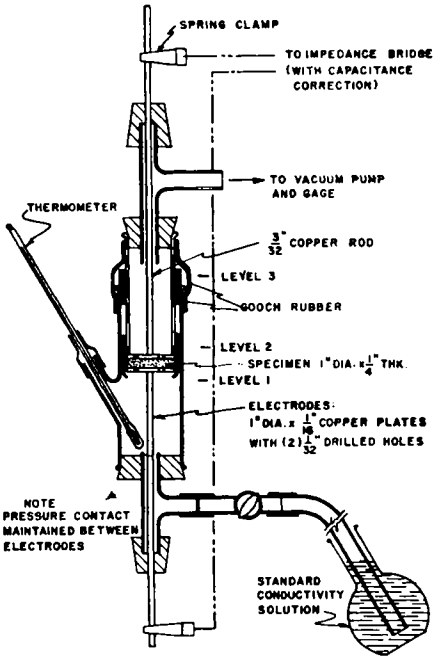

Fig. 7. Resistivity cell for porous solid specimens.

The hydraulic radiuses for fritted glass, with both water and CCl_4, are compared below:

	Coarse	Medium	Fine
m, (H_2O), μ	16.3	2.76	1.52
m, (CCl_4), μ	18.1	2.08	1.28

This indicates that CCl_4 tends to give a low reading on glass, probably because of a small angle of contact which is ignored in the equation above.

Electrical-resistivity Ratio. For nonconducting porous bodies made from such materials as ceramics and plastics, the apparatus shown in Figure 7 was used. The specimen is mounted between copper electrodes (satisfactory for K_2CO_3 solution) at the end of a 1-in. O.D. glass tube. The assembly is held together with Gooch rubber, and the electrodes are pressed tightly against the specimen. Each electrode is perforated with two small holes to permit evacuation of the specimen and saturation with an electrolyte of known electrical resistivity.

The cell is connected first to a Hyvac pump and the air exhausted. Then the electrolyte is slowly introduced until the specimen is just immersed. The water will boil a little until all the air is displaced. Then the vacuum is partially released (until boiling stops), and additional electrolyte is sucked through to sweep out any partly concentrated electrolyte present in the specimen. The vacuum is finally released altogether, the tightness of contact of electrodes is checked, and the resistance is then measured. The temperature is recorded, and the electrolyte analyzed.

For this work the Heath-Kit Model BI-Bl was used with 1,000-cycle alternating current and telephone detection. Frequently a poor null point was encountered, which was somewhat improved by use of a weaker electrolyte, i.e., about 0.1N. The capacitance

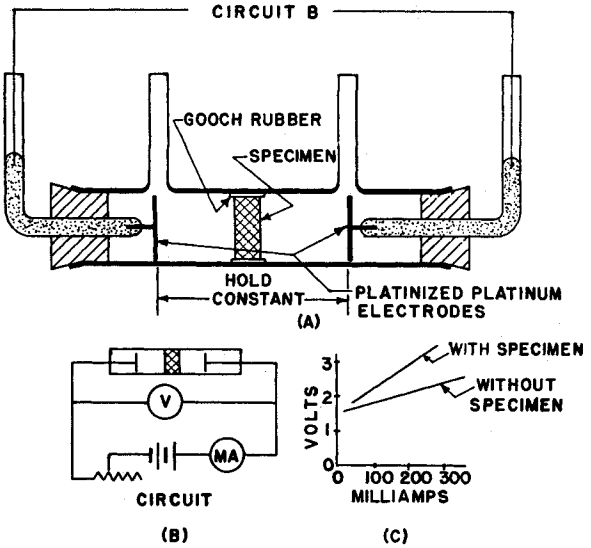

Fig. 8. Direct-current resistivity cell.

effect in the cell was then balanced out, and although this sharpened the null point, it did not appreciably affect the value of the resistance. This means that the reactance of the circuit was small, certainly under 5%.

The specific resistivity of the solution was read from the charts, the applicable concentration and temperature being used. Independent checks of the resistivity were made, and these generally checked the estimated value to within ±1 or 2%. If (r) = specific resistivity of the electrolyte, $R_0 = (r)L/A$, and from this R/R_0 is calculated.

For electrically conducting porous bodies, such as porous carbon and graphite or porous metallic membranes, a different technique is required. The porous body itself would conduct alternating current, so much more than the electrolyte that the resistance of the latter could be estimated only by subtracting two large quantities of almost equal magnitude. Therefore direct current is used, and as long as the potential difference across the membrane is appreciably less than the decomposition potential of the solution, the membrane itself provides no path for the direct current (except for a small leakage current at very low current density).

The apparatus used is shown in Figure 8. The electrodes must not be placed in contact with the specimen. Provision must be made to vent gases (H_2 and O_2) evolved at the cathode and anode. The specimen can be evacuated and saturated either before it is mounted or while it is in place. The authors favor the latter procedure. In principle, the total polarization of the cell is measured with and without the specimen in the path. During the measurements the current (a matter of milliamperes) is kept constant. Voltages are read at various currents, and the slope of the volt-ampere curve is established. A comparison of these slopes, with and without the specimen in the path, permits calculation of the R/R_0 value.

If R_1 = resistance of electrolyte with specimen in path, R_2 = resistance of electrolyte without specimen in path, and $R_0 = (r)L/A$, then

$$R/R_0 = \frac{R_1 - R_2}{R_0} + 1 \qquad (20)$$

This method for R/R_0 is not so accurate as the a.c. method previously described. The thicker the specimen in relation to the electrode spacing, the greater the precision. When both methods have been used on ceramic bodies, a comparison indicates that in most cases the d.c. method gives a somewhat lower value for R/R_0. The agreement is generally within 10%.

Nonrigid Porous Sheets

Porous sheets of polyvinyl chloride, rubber, or woven fabrics are easily tested in the apparatus shown in Figures 13* (permeability and bubble-point tests) and 14* (resistivity test). Some physically weak materials have to be supported by coarse screens to prevent bending. The sheets are sealed at the edges where clamped between the faces of the glass-spool pieces.

No new principles are involved, but a word of caution is offered in dealing with hydrophobic materials, such as polyvinyl chloride. In the resistivity measurement a wetting agent had to be added to the electrolyte to achieve 100% saturation of the pores during the evacuation and saturation procedures. Obviously the specific resistivity of solution used had to be measured, rather than calculated. In the bubble-point test no wetting agent should be used, as this would lower the surface tension of water to some indefinite value. The correct bubble-point pressure is obtained, because the same pressure is required to force water into a hydrophobic specimen, as to force the water out of a hydrophilic specimen.

EXPERIMENTAL RESULTS

The range of this experimental work is summarized in Table B. Also shown is the work of other investigators for which sufficient information is at hand to test the proposed relation. Individual points will be found plotted in Figure 10. Tables

*See footnote on page 394.

TABLE B. SUMMARY OF RESULTS SHOWN IN TABLES 1 TO 9*

(Individual points are plotted in Figure 10.)

Reference table	1	2	3	4	5	6	7	8	9	Ensemble
Experimenters	(1)	(1)	(1)	(1)	(1)	(1)	(2), (3)	(4)	(5)	
Material tested	Glass beads	Quartz sand	Porcelain	Carbon	Glass frit	PVC sheet	Glass beads	Bonded alumina	Sandstone	
Structure	Packed bed	Packed bed	Rigid	Rigid	Rigid	Flexible	Packed bed	Rigid	Rigid	
Number of sets of data	6	6	7	3	3	3	14	6	4	52
Range of properties										
Particle size, $D_p(\mu)$	148–397	207–316					156–6,100			
Sphericity, ϕ	1.00	0.63–0.70					1.00			
Porosity (macro), ϵ	0.38–0.43	0.43–0.46	0.22–0.57	0.34–0.35		0.85	0.33–0.41	0.30–0.47	0.11–0.23	
Hydraulic radius†, $m(\mu)$	20.7–41.6	18.7–27.4	0.35–25.7	8.0–17.2	1.5–16.3	1.65–4.52	15.6–706	15.5–109.2	0.50–4.45	
Permeability, $P(\mu^2)$	23.4–106.8	40.6–57.7	0.007–20.4	5.0–23.8	0.05–5.62	0.13–1.94	4.6–39,041	81–226	0.002–0.42	
Resistivity ratio, R/R_0	3.87–4.08	3.73–4.27	4.19–12.89	4.19–4.60	8.23–14.49	2.78–3.47	3.80–5.30	4.87–15.40	12.10–36.20	
Derived functions										
$k = m^2P^{-1}(R/R_0)^{-1}$										
Range	3.45–4.51	2.31–3.47	2.44–4.22	2.70–3.10	2.97–5.75	3.68–6.06	2.42–4.87	2.75–6.28	2.08–6.64	
Avg.	4.10	3.15	3.31	2.96	4.79	4.51	3.44	3.59	4.37	3.666
$\sum k$	24.62	18.90	23.14	8.86	14.38	13.53	48.19	21.53	17.47	190.62
$\sum \Delta k$	3.08	3.12	3.67	2.35	4.77	2.52	7.47	5.71	6.95	39.64
$\sum \Delta^2 k$	2.206	2.615	3.243	2.067	8.775	5.714	6.654	9.125	15.080	55.479
$k_e = \epsilon m^2 P^{-1}$ Range	5.70–10.52	3.92–6.64	5.00–11.40	4.35–7.19	7.20–13.10	8.90–19.50	3.83–7.86	9.00–16.00	6.40–18.00	
Avg.	7.20	5.63	7.76	5.85	10.64	12.60	5.41	12.40	13.10	8.100
$\sum k$	43.22	33.80	54.35	17.54	31.90	37.80	75.84	74.38	52.40	421.23

Experimenters: (1) MacMullin and Muccini; (2) Plain and Morrison; (3) LaRue and Tobias; (4) A. D. Little, Inc.; (5) Cornell and Katz
*See footnote on page 394.
†Hydraulic radius by surface-tension method throughout except for columns 7 and 8.

TABLE C. COMPARISON OF R/R_0 AS MEASURED BY PRESENT AUTHORS, WITH R/R_0 CALCULATED FROM THE EQUATION OF DE LARUE AND TOBIAS

R/R_0 as measured, for packed beds. R/R_0 as calculated from Equation (21), which applies to random dispersions of floating particles.

Col.	ϵ	R/R_0 calc.	R/R_0 meas.	% Dev.
Glass beads (*See* Table 1)				
1	0.3835	4.20	3.993	+ 5.3
2	0.4183	3.70	4.000	− 7.5
3	0.4268	3.56	3.900	− 6.1
4	0.4247	3.60	3.876	− 7.1
5	0.3975	3.98	4.085	− 2.6
6	0.4056	3.88	4.083	− 5.0
			Average	− 3.8
Sand (*See* Table 2)				
8	0.4470	3.32	4.050	−18.0
9	0.4470	3.32	4.275	−22.3
10	0.4325	3.50	3.992	−12.3
11	0.4356	3.47	3.920	−11.5
12	0.4570	3.21	3.730	−13.9
			Average	−15.6

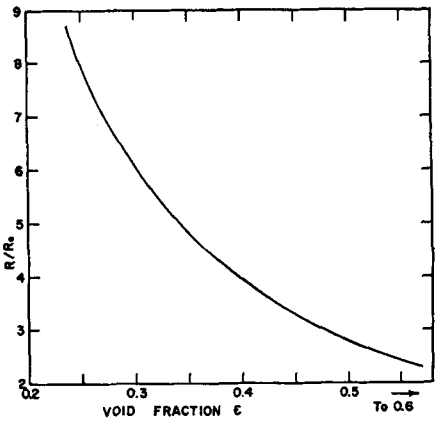

Fig. 9. Resistivity ratios of random dispersions; plot of De LaRue-Tobias equation $R/R_0 = \epsilon^{-3/2}$.

1 to 9* contain the results of individual sets of data.

ADDITIONAL EVIDENCE

Resistivity Ratio as a Function of Void Fraction

De LaRue and Tobias (*12*) have measured the fractional decrease in conductivity of a fluid medium resulting from random suspensions of various nonconducting particles in the fluid. The particles tested include glass spheres, polystyrene cylinders, and sand, of varying sizes. These were suspended in an aqueous solution of $ZnBr_2$ of approximately the same density as the particles, the slurry then being agitated to give random dispersions. The volume fraction of dispersed phase ranged from zero to a value approaching that for loosely packed beds. The authors found the following relation to hold, to a high degree of precision:

$$R/R_0 = \epsilon^{-3/2} \qquad (21)$$

The relation is plotted in Figure 9.

Now arises the question of whether this equation has validity when extrapolated to the region corresponding to packed beds, where all the particles are more or less in intimate contact with surrounding particles. The answer is seen in the data presented in Table C. One concludes that the De LaRue-Tobias equation gives consistently low values for R/R_0 but is good to about 4% for packed beds of glass spheres. For packed beds of irregular grains, the equation can not be depended upon, even as an approximation. The equation cannot be used at all for consolidated porous bodies.

Glass Beads

Plain and Morrison (*20*) measured the flow permeability of fourteen media composed of packed spherical glass beads, using the Terzaghi method. By using three fluids of widely different viscosity, they were able to determine the limits of viscous flow in terms of a critical Reynolds number.

In their Table I porosity ϵ and sphere diameter D are given from which has been calculated hydraulic radius by the relation $m = D\epsilon\phi/6(1 - \epsilon)$. Several values for permeability P are given, and those values demonstrably within the viscous-flow range were selected. Since Plain and Morrison did not measure the resistivity ratio R/R_0, the present authors have estimated it, using the De LaRue-Tobias relation, Equation (12), which has just been shown to be applicable to unconsolidated packed beds of spheres. This information is detailed in Table 7, summarized in Table B, and plotted in Figure 10.

The results support the proposed Equation (1) very well and give a mean value of $k = 3.44$.

Bonded Porous Alumina

A series of measurements on porous materials was carried out by A. D. Little, Inc. (*18*). Among the properties measured were porosity, air permeability, and electrical-resistivity ratio. No attempt was made to measure hydraulic radius directly. However, among the materials tested were six samples of porous bonded 85% alumina bodies, for which the manufacturer (Norton Company) supplies accurate data as to grain size before bonding. The grain size had been determined by microscope, with the average results given in Table 8. The manufacturer also estimated sphericity of grains (before bonding) as $\phi = 0.80$. During firing, the bond spreads and tends to round off the grains and broaden the points of contact, thus causing cementation. This increases the sphericity to an estimated $\phi = 0.90$. The hydraulic radius m of the bonded specimen can then be estimated. Sufficient data were available to calculate P and R/R_0.

This information is detailed in Table 7, summarized in Table B, and plotted in Figure 10. The results support the proposed Equation (1) very well and give a mean value of $k = 3.59$.

Sandstone

Cornell and Katz (*11*) measured the porosity, gas permeability, and resistivity ratio for twenty-four different samples of sandstone, dolomite, and limestone. The samples covered a wide range of these properties. Gas flow was in most cases in the viscous-turbulent region, and the pressure drop through the specimens was of considerable magnitude. Equations were developed to segregate the viscous-flow contribution α from the turbulent flow contribution β to the total permeability. Suitable corrections were made for gas expansion within the sample.

Only a few specimens were tested for equivalent pore size (diameter of circular capillary having same viscous-flow permeability). In their Figure I they show distribution of equivalent pore size vs. accumulative percentage of the total voids smaller than this size. No details of the method are given, other than that it was based on the water displaced from saturated specimens as air pressure was applied to the specimen.

The authors did not make any direct measurements of hydraulic radius m or equivalent pore size. In handling their data, they used a modified form of the Kozeny-Carman relation, given in their Equation (10).

Noting that $D_E = 4m$ for a circular capillary of uniform crosssection and that the authors arbitrarily take $k_1 = 0.50$, one finds that this equation reduces to

$$m^2 = \frac{4uL\eta}{\Delta p\, g} \cdot \frac{R}{R_0} = 4PR/R_0 \qquad (22)$$

This is identical with Equation (1) save for the numerical coefficient. Thus Cornell and Katz assumed a coefficient of 4 as being of the right order of magnitude (a very close approximation), whereas the

*See footnote on page 394.

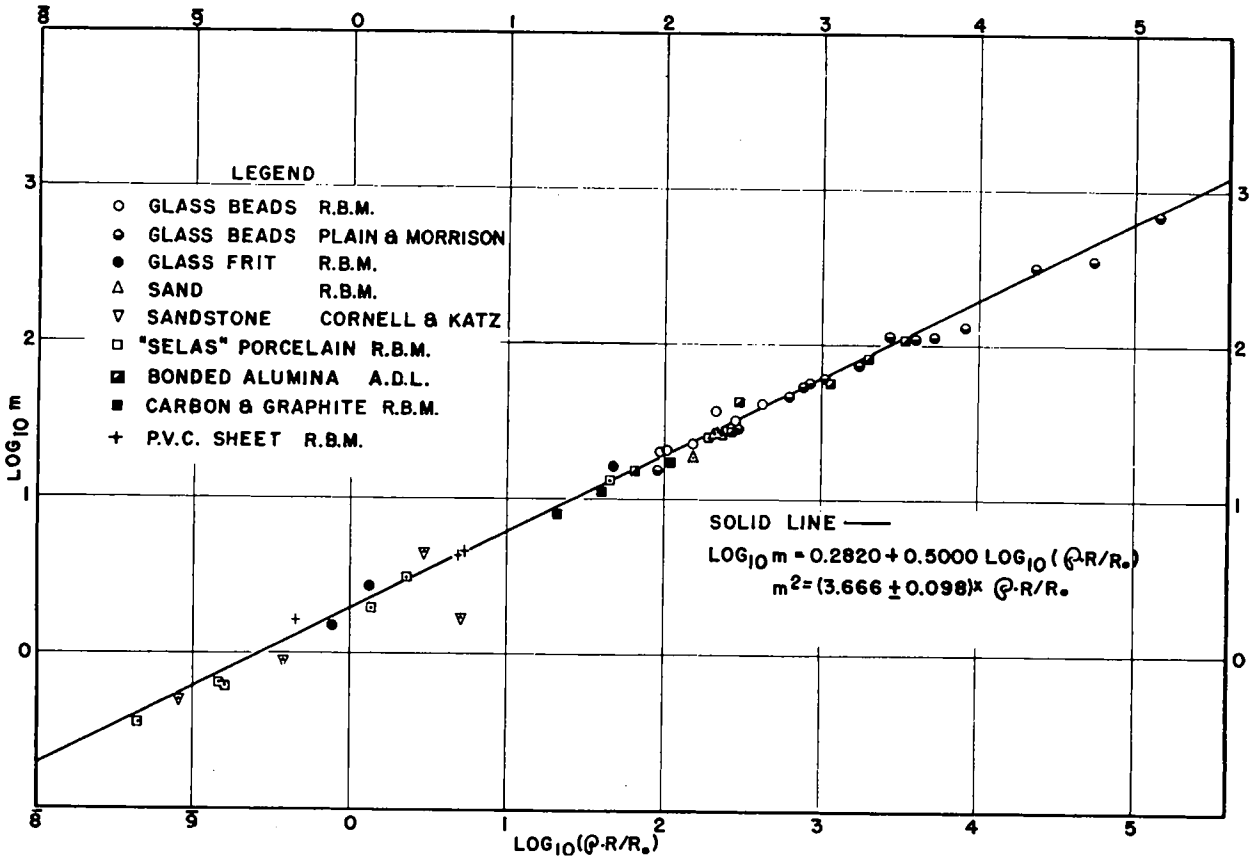

Fig. 10. Correlation plot for MacMullin equation $m^2 = kPR/R_0$.

present authors have experimentally determined this coefficient as being 3.666 ± 0.098. The results given by Cornell and Katz in their Table III all fall exactly on the curve represented by Equation (22) since D_E (or m) was calculated by means of this relation.

MacMullin and Muccini have calculated m from the pore size distribution curves in Cornell and Katz's Figure I, for the four samples of sandstone for which this was measured. Since fine pores contribute more to m than do coarse pores, the effective hydraulic radius must be the reciprocal average value of m. For equal increments of total void fraction,

$$m(\text{recip. avg.}) = \frac{1}{\Sigma(1/m)} \quad (23)$$

The method of calculation is detailed in Table 10.

The results are detailed in Table 9, summarized in Table B, and plotted in Figure 10. The data deviate widely (both plus and minus) from the expected values, although the average value of $k = 4.37$ is not far from the expected value, $k = 3.67$. This fact emphasizes the desirability of direct experimental determination of hydraulic radius by reliable methods.

DISCUSSION OF RESULTS

It was first necessary to establish the validity of the break-point and bubble-point methods for the measurement of hydraulic radius. The data on glass beads, Table 1, indicate an approximate concordance between m (breakpoint) and m (D and ϵ). Agreement is closest for uniformly sized beds, but m (breakpoint) gives high results for beds of mixed sizes.

MacMullin and Muccini believe that their experimentally determined values of m have real meaning with respect to permeability. These values of m may not always be strictly the same as those based on true values for total specific voids and total specific surface, but they reflect the fact that some of the surface may be blanked off, contributing nothing to support of the sealing liquid in the break-point method or to drag in permeability measurement.

The justification for use of surface-tension methods of determining hydraulic radius rests on the demonstration that these methods can be applied to all manner of porous media with reasonably consistent results.

The work on sand, Table 2, was preceded by many measurements on break-point only, to arrive at the effective specific surface of each cut of sand and thus to arrive at the sphericity ϕ of the sand in the permeability measurements. Independent measurements of sphericity all checked closely, and the average value was used to check the m values found in the flow experiments. The close checks in all cases merely indicate the reproducibility of the break-point method and are not any inherent check on the "true" value of m.

All the rest of the work was done on consolidated porous media, such as Selas porcelain, Table 3; carbon and graphite, Table 4; fritted glass, Table 5; and polyvinyl chloride sheet, Table 6.

To these experimental results are added the calculated results based on the work of others, as for example, glass beads, Table 7; bonded alumina, Table 8; and sandstone, Table 9. Thus one is able to double the number of experimental data which can be used to test the validity of the proposed relation, $m^2 = kPR/R_0$. Out of a total of fifty-two sets of data, twenty-eight are contributed by MacMullin and Muccini.

The authors wish to point out that in their work each set of results represents the average of several independent checks on m, P, and R/R_0, alternative fluids and methods being frequently used for these tests. They are sure that in all cases the permeability measurements that they made were in the viscous-flow range, well below the critical Reynolds number.

The entire fifty-two sets of results are plotted in Figure 10, log m vs. log PR/R_0. To be dimensionally consistent, the straight line through these points must have a slope of 0.50. The position of the line was determined by least square methods.

In each column of each table is recorded the constant k of the equation, $m^2 = kPR/R_0$, the deviation from the mean $k = 3.666$, and the square of the deviation. Using the relations

probable error of the mean

$$E(k) = \frac{0.6745}{\sqrt{(n(n-1)}} \sqrt{\Sigma \Delta^2 k}$$

probable error of single observation,

$$e(k) = \frac{0.6745}{\sqrt{n-1}} \sqrt{\Sigma \Delta^2 k}$$

one finds the following:

	Experimental work columns 1–26	Whole array columns 1–52
k (mean)	3.690	3.666
$E(k)$	0.122 (3.3%)	0.098 (2.7%)
$e(k)$	0.646 (17.6%)	0.703 (19.2%)

The authors are satisfied with the accuracy of the mean value of k, although the probable error of any single set, when their technique is used, is as high as 0.646, or 17.6%. The expected error therefore in calculating any one of the three parameters m^2, P, R/R_0 from the other two is 17.6%. The expected error in calculating m from P and R/R_0, however, is only half this, or 8.8%. The expected error in estimating effective specific surface ($s = \epsilon/m$) is about 10%.

To test the alternative correlation of Kozeny-Carman, they have listed $k_c = \epsilon m^2 P^{-1}$ in the tables. For packed beds only,

	Experimental work columns 1–12	Plain and Morrison columns 29–42	Whole array (26 points)
k_c	6.15	5.42	5.76

Carman himself recommended the value $k_c = 5$, although many other workers seem to prefer a value of $k_c = 5.5$. Thus, the Kozeny-Carman correlation for packed beds is verified. However, inspection of the tables for consolidated porous media reveals a wide deviation, k_c reaching values as high as 18 on some samples of sandstone.

The new correlation does not hold for straight-walled capillaries, for which $R/R_0 = 1$, and $m^2 = k_0 P$. In such cases $k_0 = 2.0$ for round capillaries (Poiseuille's law) and may range from 1.2 to 3.0 for other than round cross sections. For porous media the constant $k = 3.666$ appears to be outside this range.

The new correlation covers a thousandfold range of hydraulic radius and a millionfold range in permeability; it covers a wide range of types of porous media, including packed granular beds and both rigid and flexible consolidated media, and the correlation is independent of the porosity, which covers a range of $\epsilon = 0.1$ to $\epsilon = 0.85$. This would seem to justify the use of this correlation, even though it lacks some desired precision.

Reynolds Number

Since *pore diameter* has no meaning within a porous body, the Reynolds number can be written in terms of the effective hydraulic radius m,

$$Re = \frac{m u_e \rho}{\eta} \qquad (24)$$

where u_e is the "effective" velocity within the porous body. One recognizes that this velocity varies from point to point, just as m does.

It has been pointed out by Carman (*6*) and others that if L_e = the effective length of path of fluid through the bed and u = the superficial velocity of the fluid then

$$u_e = \frac{u}{\epsilon} \cdot \frac{L_e}{L} \qquad (25)$$

Likewise it can be shown that

$$\frac{R}{R_0} = \frac{1}{\epsilon} \left(\frac{L_e}{L}\right)^2 \qquad (26)$$

Combining Equations (25) and (26) gives

$$u_e = u \left(\frac{R/R_0}{\epsilon}\right)^{1/2} \qquad (27)$$

Substituting in (24) yields

$$Re = \frac{mu\rho}{\eta} \cdot \left(\frac{R/R_0}{\epsilon}\right)^{1/2} \qquad (28)$$

Plain and Morrison (20) defined their Reynolds number differently:

$$Re' = \frac{D_p u_e \rho}{\eta} \qquad (29)$$

In their experiments on glass beads they arbitrarily take

$$L_e/L = \sqrt{2.5} = 1.58,$$

so that

$$u_e' = \frac{u}{\epsilon} \cdot 1.58$$

Also,

$$m = \frac{\epsilon}{1-\epsilon} \frac{D_p}{6} \text{ (for beds of spheres)}$$

and one can use the LaRue-Tobias realtion

$$R/R_0 = \epsilon^{-3/2} \text{ (for beds of spheres)}$$

Combining yields

$$Re = \frac{\epsilon}{1-\epsilon} \cdot \frac{1}{6} D_p \cdot u_e' \cdot \frac{\epsilon}{1.58} \cdot \frac{\rho}{\eta} \cdot \left(\frac{\epsilon^{-3/2}}{\epsilon}\right)^{1/2}$$

$$= \frac{1}{9.48} \cdot \frac{\epsilon^{3/4}}{1-\epsilon} \cdot Re' \qquad (30)$$

As Plain and Morrison reached a critical Reynolds number, $Re' = 75$ in their bed 9, for which ϵ was 0.35,

$$Re_{crit} = \frac{1}{9.48} \cdot \frac{(0.35)^{3/4}}{0.65} \cdot 75 = 5.54$$

Carman (*6*) defines the Reynolds number

$$Re'' = \frac{\rho u}{\eta s} = \frac{mu\rho}{\epsilon\eta} \qquad (31)$$

Therefore

$$Re = (\epsilon R/R_0)^{1/2} \cdot Re'' \qquad (32)$$

For random-packed beds, where ϵ approximates 0.40 and R/R_0 approximates 4.0, then

$$Re = (0.4 \times 4)^{1/2} Re'' = 1.265\, Re''$$

Carman gives the critical Reynolds number as $Re''_{crit} = 2$; hence

$$Re_{crit} = 1.265 \times 2 = 2.53$$

Chilton (*10*) defines the Reynolds number as

$$Re''' = \frac{D_p u \rho}{\eta} = \frac{6m(1-\epsilon)}{\phi\epsilon} \cdot \frac{u\rho}{\eta} \qquad (33)$$

Thus

$$Re = \frac{\phi\epsilon}{6(1-\epsilon)} \cdot \left(\frac{R/R_0}{\epsilon}\right)^{1/2} Re''' \qquad (34)$$

For random-packed spheres ϵ will average 0.4, R/R_0 4.0, and $\phi = 1.0$, and so

$$Re = \frac{0.4}{6(0.6)} \left(\frac{4}{0.4}\right)^{1/2} \cdot Re'''$$

$$= 0.325\, Re'''$$

Chilton gives the critical Reynolds number as $Re'''_{crit} = 20$. Hence, $Re_{crit} = 0.325 \times 20 = 6.50$.

Summing up, MacMullin and Muccini prefer to use the Plain and Morrison data on critical Reynolds number, as they were aimed specifically at determining its value; that is, $Re_{crit} = 5.5$, and below this value 100% viscous flow prevails.

Friction Factor

In the viscous-flow region the product of the friction factor and the Reynolds number must be a constant, in order that u be proportional to Δp; that is,

$$f \times Re = \frac{m^2}{PR/R_0} = 3.666 \qquad (35)$$

Substituting the value of Re [Equation (28)],

$$f = \frac{m\eta\epsilon^{1/2}}{Pu\rho(R/R_0)^{3/2}} \qquad (36)$$

and breaking down P into its components yields

$$f = \frac{m\,\Delta p\, g}{u^2 L \rho} \cdot \frac{\epsilon^{1/2}}{(R/R_0)^{3/2}} \qquad (37)$$

This form of the friction factor differs from that of Carman, who gives

$$f'' = \frac{m\,\Delta p\, g}{u^2 L \rho} \cdot \epsilon^2 \qquad (38)$$

As a special case, for packed beds of spheres, one may apply the LaRue-Tobias

relation $(R/R_0) = \epsilon^{-3/2}$, and Equation (37) takes the form

$$f = \frac{m\,\Delta p\,g}{u^2 L \rho}\cdot\epsilon^{9/4} \qquad (37a)$$

which is practically identical with Equation (38).

The subject of this paper is limited to flow in the viscous region. It is suggested, however, that a new plot of f vs. Re, as defined by Equations (28) and (37), would yield rewarding results. In this paper the proper location of the plot in the viscous-flow region and the approximate point of departure where turbulent flow begins to take over have been established. In order for the new equations to be valid, it is recognized that the hydraulic radius, as defined, is an experimentally determined property, based on surface-tension phenomena. Where it has been possible to check m from particle size, sphericity, and porosity measurements, the agreement has been tolerably good.

NOTATION

		Dimensions
A	= cross-sectional area of specimen	l^2
a	= cross-sectional area of liquid column in the Terzaghi method for liquid permeability	l^2
C	= pressure-correction factor in measurement of permeability to gas flow	0
D	= particle diameter	l
D_{ra}	= reciprocal average particle diameter	l
d	= density of solid part of specimen	ml^{-3}
E	= voltage drop through specimen	volts
$E(k)$	= probable error of the mean value of k	0
$e(k)$	= probable error of a single determination of k	0
f	= friction factor	0
g	= acceleration of gravity	lt^{-2}
h	= static head of fluid	l
H	= hydraulic head in Terzaghi's method for permeability	l
I	electric current	amp.
I_0	= current density on superficial area of specmen	amp. l^{-2}
k	= coefficient in MacMullin equation for permeability	0
k_c	= coefficient in Kozeny-Carman equation for permeability	0
L	= thickness of specimen in direction of gradient	l
L_e	= effective length of path of fluid in traversing specimen	l
m	= hydraulic radius of specimen, ratio of specific voids to specific surface ϵ/s	l
$\bar{m}$	= mean effective value of m for permeability	l
N	= normality, gram equivalents per liter	ml^{-3}
P	= permeability coefficient of specimen	l^2
p	= pressure	ml^{-2}
R	= electrical resistance	ohms
R/R_0	= electrical-resistivity ratio, a property of the specimen	0
Re	= Reynolds number	0
(r)	= specific electrical resistance	ohms l
s	= specific surface (macroscopic) of porous bed	l^{-1}
s'	= specific surface of (nonporous) particles in bed	l^{-1}
t	= time	t
u	= velocity; unless otherwise noted, the superficial fluid velocity through a unit cross section of specimen in direction of gradient	lt^{-1}
u_e	= effective, or local, velocity of fluid in pores of specimen	lt^{-1}
V	= gross volume of porous specimen	l^3
w	= weight of specimen	m
x	= distance in specimen, measured in direction of gradient	l
x_a	= head of liquid supported in break-point method	l
y	= liquid removed from bed, as measured in level tube, in break-point method	l
z	= specific viscosity relative to water	0
γ	= surface tension	mt^{-2}
Δk	= deviation from the mean value of k	0
ϵ	= void fraction of specimen (total voids)	0
ϵ_{ma}	= macrovoid fraction (exterior to particles of bed)	0
ϵ_{mi}	= microvoid fraction (interior of particle of bed)	0
η	= viscosity of fluid	$ml^{-1}t^{-1}$
θ	= angle of contact of fluid with solid part of specimen	degrees
κ	= specific electrical conductance	ohm$^{-1}l^{-1}$
μ	= microns, 10^{-4} cm.	l
Π	= permeability to a particular fluid, where $\Pi = uL\Delta p^{-1}$	$m^{-1}l^4t^{-1}$
ρ	= density of fluid	ml^{-3}
ϕ	= sphericity of particle, $6/(Ds')$	0
χ	= tortuosity function	0

LITERATURE CITED

1. Archie, G. E., *Trans. Am. Inst. Mining Met. Engrs.*, **146**, 54 (1942).
2. Brownell, L. E., and D. L. Katz, *Chem. Engr. Progr.*, **43**, 537 (1947).
3. *Ibid.*, **43**, 601 (1947).
4. *Ibid.*, p. 703.
5. Brownell, L. E., D. C. Gami, R. A. Miller, and W. F. Nekarvis, *A.I.Ch.E. Journal*, **2**, No. 1, 79 (1956).
6. Carman, P. C., *Trans. Inst. Chem. Engrs. (London)*, **15**, 150 (1937).
7. *Ibid.*, **16**, 168 (1938).
8. *Ibid.*, **27**, 237 (1949).
9. Carman, P. C., *J. Soc. Chem. Ind.*, **69**, 134 (1950).
10. Chilton, T. H., and A. P. Colburn, *Trans. Am. Inst. Chem. Engrs.*, **26**, 178 (1931).
11. Cornell, D., and D. L. Katz, *Ind. Eng. Chem.*, **45**, 2145 (1953).
12. De LaRue, R. E., and C. W. Tobias, Paper 181, presented at Cincinnati meeting of Electrochem. Soc. (May 1–5, 1955).
13. Dallavalle, J. M., "Micromeritics," 2 ed., Pitman Publishing Corp., Chicago (1948).
14. Ergun, S. K., *Chem. Eng. Progr.*, **48**, 89 (1952).
15. Grace, H. P., *loc. cit.*, **49**, 303 (1953).
16. Hatfield, M. R., *Ind. Eng. Chem.*, **31**, 1419 (1939).
17. Leva, Max et al., *U.S. Bur. Mines Bull.* 504 (1951).
18. Little, Arthur D., Inc., *Rept. C-58493* (1953); private communication to R. B. MacMullin.
19. Muskat, Irving, "Flow of Homogeneous Fluids Through Porous Media," McGraw-Hill Book Company, Inc., New York (1937).
20. Plain, G. J., and H. L. Morrison, *Am. J. Phys.*, **22**, 143 (1954).
21. Rudolph, Hans, *Kolloid Z.*, **67**, 93 (1934).
22. Samartsev, A. G., and V. V. Ostroumov, *Kolloid Zhur.*, **12**, 136 (1950).
23. Sauer, M. C., P. F. Southwick, K. S. Spiegler, and M. R. Wyllie, *Ind. Eng. Chem.*, **47**, 2187 (1955).
24. Scheidegger, A. E., *J. Appl. Phys.*, **25**, 994 (1954).
25. Slawinsky, A., *J. Chim. Phys.*, **23**, 710 (1926).
26. Terzaghi, Karl, and R. B. Peck, "Soil Mechanics," John Wiley & Sons, Inc., New York (1948).
27. Tiller, F. M., *Chem. Eng. Progr.*, **49**, 467 (1953).
28. *Ibid.*, **51**, 282 (1955).
29. Velisek, von J., and A. Vasicek, *Kolloid Z.*, **71**, Heft. 1, 36 (1935).
30. Wagstaff, J. B., and E. A. Nirmaier, *Ind. Eng. Chem.*, **47**, 1129 (1955).
31. Whitney, R. P., W. L. Ingmanson, and S. T. Han, *Trans. Am. Paper Pulp Inst.*, **38**, 157 (1955).
32. Wirth, J. K., *Kolloid Z.*, **116**, 47 (1950).
33. Wyllie, M. R., and A. R. Gregory, *Trans. Am. Inst. Mining Met. Engr.*, **198**, 103 (1953).
34. ———, *Ind. Eng. Chem.*, **47**, 1379 (1955).
35. Zhukov, I. I., and D. A. Fridrikhsberg, *Kolloid Zhur.*, **11**, 163 (1949).